
You Only Look Once: Unified, Real-Time Object Detection

000
001
002
003
004
005
006
007
008
009
010
011
012
013
014
015
016
017
018
019
020
021
022
023
024
025
026
027
028
029
030
031
032
033
034
035
036
037
038
039
040
041
042
043
044
045
046
047
048
049
050
051
052
053
Anonymous Author(s)

Affiliation
Address
email

Abstract

We present YOLO, a unified pipeline for object detection. Prior work on object detection repurposes classifiers to perform detection. Instead, we frame object detection as a regression problem to spatially separate bounding boxes and associated class probabilities. A single neural network predicts bounding boxes and class probabilities directly from full images in one evaluation. Since the whole detection pipeline is a single network, it can be optimized end-to-end directly on detection performance. Our unified architecture is also extremely fast; YOLO processes images in real-time at 45 frames per second, hundreds to thousands of times faster than existing detection systems. Our system uses global image context to detect and localize objects, making it less prone to background errors than top detection systems like R-CNN. By itself, YOLO detects objects at unprecedented speeds with moderate accuracy. When used in combination with state-of-the-art detectors, YOLO boosts performance by 2-3% points mAP.

1 Introduction

Humans glance at an image and instantly know what objects are in the image, where they are, and how they interact. The human visual system is fast and accurate, allowing us to perform complex tasks like driving or grocery shopping with little conscious thought. Fast, accurate, algorithms for object detection would allow computers to drive cars in any weather without specialized sensors, enable assistive devices to convey real-time scene information to human users, and unlock the potential for general purpose, responsive robotic systems.

Convolutional neural networks (CNNs) achieve impressive performance on classification tasks at real-time speeds [13]. Yet top object detection systems like R-CNN take seconds to process individual images and hallucinate objects in background noise. We believe these shortcomings result from how these systems approach object detection.

Current detection systems repurpose classifiers to perform detection. To detect an object these systems take a classifier for that object and evaluate it at various locations and scales in a test image. Systems like deformable parts models (DPM) use a sliding window approach where the classifier is run at evenly spaced locations over the entire image [7]. More recent approaches like R-CNN use region proposal methods to first generate potential bounding boxes in an image and then run a classifier on these proposed boxes. After classification, post-processing is used to refine the bounding box, eliminate duplicate detections, and rescore the box based on other objects in the scene [9].

These region proposal techniques typically generate a few thousand potential boxes per image. Selective Search, the most common region proposal method, takes 1-2 seconds per image to generate these boxes [26]. The classifier then takes additional time to evaluate the proposals. The best performing systems require 2-40 seconds per image and even those optimized for speed do not achieve real-time performance. Additionally, even a highly accurate classifier will produce false positives

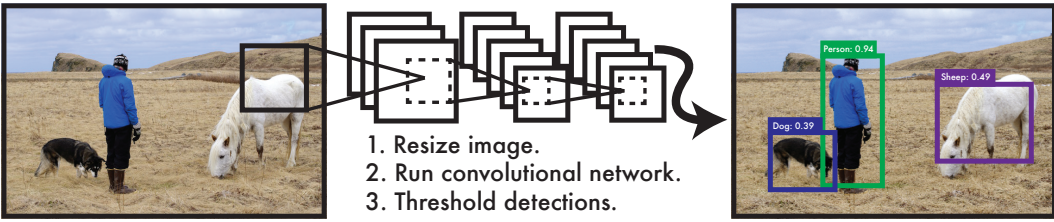


Figure 1: The YOLO Detection System. Processing images with YOLO is simple and straightforward. Our system (1) resizes the input image to 448×448 , (2) runs a single convolutional network on the image, and (3) thresholds the resulting detections by the model’s confidence.

when faced with so many proposals. When viewed out of context, small sections of background can resemble actual objects, causing detection errors.

Finally, these detection pipelines rely on independent techniques at every stage that cannot be optimized jointly. A typical pipeline uses Selective Search for region proposals, a convolutional network for feature extraction, a collection of one-versus-all SVMs for classification, non-maximal suppression to reduce duplicates, and a linear model to adjust the final bounding box coordinates. Selective Search tries to maximize recall while the SVMs optimize for single class accuracy and the linear model learns from localization error.

Our system is refreshingly simple, see Figure 1. A single convolutional network simultaneously predicts multiple bounding boxes and class probabilities for those boxes. We train our network on full images and directly optimize detection performance. Context matters in object detection. Our network uses global image features to predict detections which drastically reduces its errors from background detections. At test time, a single network evalution of the full image produces detections of multiple objects in multiple categories without any pre or post-processing.

Our training and testing code are open source and available online at [redacted]. A variety of pre-trained models are also available to download.

2 Unified Detection

We unify the separate components of object detection into a single neural network. Using our system, you only look once (YOLO) at an image to predict what objects are present and where they are. Our network uses features from the entire image to predict each bounding box. It also predicts all bounding boxes for an image simultaneously. This means our network reasons globally about the full image and all the objects in the image. The YOLO design enables end-to-end training and real-time speeds while maintaining high average precision.

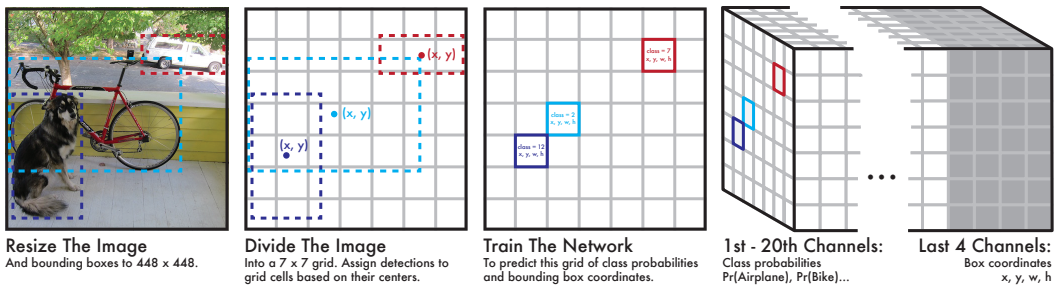


Figure 2: The Model. Our system models detection as a regression problem to a $7 \times 7 \times 24$ tensor. This tensor encodes bounding boxes and class probabilities for all objects in the image.

108
109

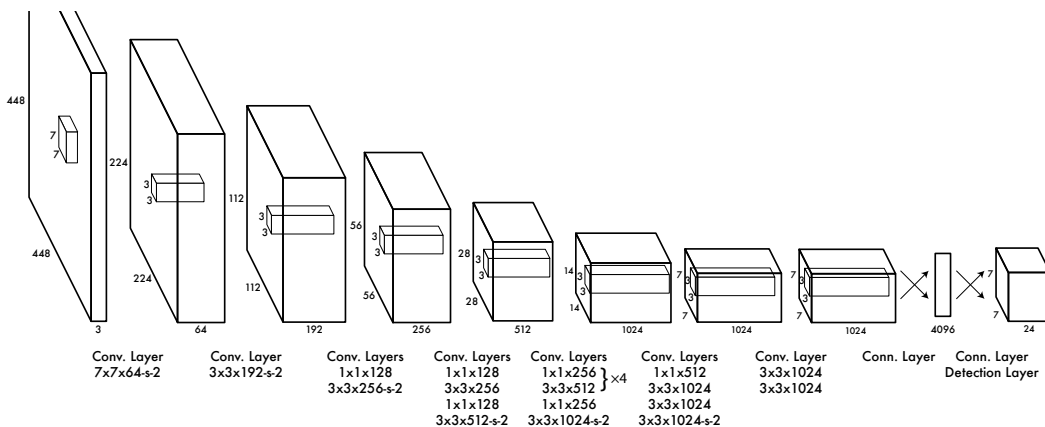
2.1 Design

110 Our system divides the input image into a 7×7 grid. If the center of an object falls into a grid cell,
111 that grid cell is responsible for detecting that object. Each grid cell predicts a bounding box and
112 class probabilities associated with that bounding box, see Figure 2.

113 We implement this model as a convolutional neural network and evaluate it on the PASCAL VOC
114 detection dataset [6]. The initial convolutional layers of the network extract features from the image
115 while the fully connected layers predict the output probabilities and coordinates.

116 Our network architecture is inspired by the GoogLeNet model for image classification [25]. Our
117 nework has 24 convolutional layers followed by 2 fully connected layers. However, instead of the
118 inception modules used by GoogLeNet we simply use 1×1 reduction layers followed by 3×3
119 convolutional layers, similar to Lin et al [17]. We also replace maxpooling layers with strided
120 convolutions. The full network is shown in Figure 3.

121 The final output of our network is a 7×7 grid of predictions. Each grid cell predicts 20 conditional
122 class probabilities, and 4 bounding box coordinates.
123



138 **Figure 3: The Architecture.** Our detection network has 24 convolutional layers followed by 2 fully
139 connected layers. The network uses strided convolutional layers to downsample the feature space
140 instead of maxpooling layers. Alternating 1×1 convolutional layers reduce the features space from
141 preceding layers. We pretrain the convolutional layers on the ImageNet classification task at half
142 the resolution (224×224 input image) and then double the resolution for detection.

143

2.2 Training

144 We pretrain our convolutional layers on the ImageNet 1000-class competition dataset [22]. For
145 pretraining we use the first 20 convolutional layers from Figure 3 followed by a maxpooling layer
146 and two fully connected layers. We train this network for approximately a week and achieve a top-5
147 accuracy of 86% on the ImageNet 2012 validation set.

148 We then adapt the model to perform detection. Ren et al. show that adding both convolutional and
149 connected layers to pretrained networks can benefit performance [21]. Following their example,
150 we add four convolutional layers and two fully connected layers with randomly initialized weights.
151 Detection often requires fine-grained visual information so we increase the input resolution of the
152 network from 224×224 to 448×448 .

153 Our final layer predicts both class probabilities and bounding box coordinates. We normalize the
154 bounding box width and height by the image width and height so that they fall between 0 and 1. We
155 parameterize the bounding box x and y coordinates to be offsets of a particular grid cell location
156 so they are also bounded between 0 and 1. We use a logistic activation function to reflect these
157 constraints on the final layer. All other layers use the following leaky rectified linear activation:
158

$$\phi(x) = \begin{cases} 1.1x, & \text{if } x > 0 \\ .1x, & \text{otherwise} \end{cases} \quad (1)$$

162 We optimize for sum-squared error in the output of our model. We use sum-squared error because
 163 it is easy to optimize, however it does not perfectly align with our goal of maximizing average
 164 precision. It weights localization error equally with classification error which may not be ideal. To
 165 remedy this, we use a scaling factor λ to adjust the weight given to error from coordinate predictions
 166 versus error from class probabilities. In our final model we use the scaling factor $\lambda = 4$.

167 Sum-squared error also equally weights errors in large boxes and small boxes. Our error metric
 168 should reflect that small deviations in large boxes matter less than in small boxes. To partially
 169 address this we predict the square root of the bounding box width and height instead of the width
 170 and height directly.

171 If cell i predicts class probabilities $\hat{p}_i(\text{aeroplane}), \hat{p}_i(\text{bicycle})\dots$ and the bounding box $\hat{x}_i, \hat{y}_i, \hat{w}_i, \hat{h}_i$
 172 then our full loss function for an example is:

$$173 \\ 174 \\ 175 \sum_{i=0}^{48} \left(\lambda \mathbb{1}_i^{\text{obj}} ((x_i - \hat{x}_i)^2 + (y_i - \hat{y}_i)^2 + (\sqrt{w_i} - \sqrt{\hat{w}_i})^2 + (\sqrt{h_i} - \sqrt{\hat{h}_i})^2) + \sum_{c \in \text{classes}} (p_i(c) - \hat{p}_i(c))^2 \right) \quad (2)$$

176 Where $\mathbb{1}_i^{\text{obj}}$ encodes whether any object appears in cell i . Note that if there is no object in a cell we
 177 do not consider any loss from the bounding box coordinates predicted by that cell. In this case, there
 178 is no ground truth bounding box so we only penalize the associated probabilities with that region.

179 We train the network for about 120 epochs on the training and validation data sets from PASCAL
 180 VOC 2007 and 2012 as well as the test set from 2007, a total of 21k images. Throughout training
 181 we use a batch size of 64, a momentum of 0.9 and a decay of 0.0005. We use two learning rates
 182 during training: 10^{-2} and 10^{-3} . Training diverges if we use the higher learning rate, 10^{-2} , from
 183 the start. We use the lower rate, 10^{-3} , for one epoch so that the randomly initialized weights in the
 184 final layers can settle to reasonable values. Then we train with the following learning rate schedule:
 185 10^{-2} for 80 epochs, and 10^{-3} for 40 epochs.

186 To avoid overfitting we use dropout and extensive data augmentation. A dropout layer with rate = .5
 187 after the first connected layer prevents co-adaptation between layers [14]. For data augmentation we
 188 introduce random scaling and translations of up to 10% of the original image size. We also randomly
 189 adjust the exposure and saturation of the image by up to a factor of 2.

190 2.2.1 Parameterizing Class Probabilities

191 Each grid cell predicts class probabilities for that area of the image. There are 49 cells with a possible
 192 20 classes each yielding 980 predicted probabilities per image. Most of these probabilities will be
 193 zero since only a few objects appear in any given image. Left unchecked, this imbalance pushes all
 194 of the probabilities to zero, leading to divergence during training.

195 To overcome this, we add an extra variable to each grid location, the probability that any object exists
 196 in that location regardless of class. Thus instead of 20 class probabilities we have 1 “objectness”
 197 probability, $\text{Pr}(\text{Object})$, and 20 conditional probabilities: $\text{Pr}(\text{Airplane}|\text{Object})$, $\text{Pr}(\text{Bicycle}|\text{Object})$,
 198 etc.

199 To get the unconditional probability for an object class at a given location we simply multiply the
 200 “objectness” probability by the conditional class probability:

$$201 \\ 202 \text{Pr}(\text{Dog}) = \text{Pr}(\text{Object}) * \text{Pr}(\text{Dog}|\text{Object}) \quad (3)$$

203 We can optimize these probabilities independently or jointly using a novel “detection layer” in our
 204 convolutional network. During the initial stages of training we optimize them independently to
 205 improve model stability. We update the “objectness” probabilities at every location however we
 206 only update the conditional probabilities at locations that actually contain an object. This means
 207 there are far fewer probabilities getting pushed towards zero.

208 During later stages of training we optimize the unconditioned probabilities by performing the re-
 209 quired multiplications in the network and calculating error based on the result.

216 **2.2.2 Predicting IOU**
217

218 Like most detection systems, our network has trouble precisely localizing small objects. While it
219 may correctly predict that an object is present in an area of the image, if it does not predict a precise
220 enough bounding box the detection is counted as a false positive.

221 We want YOLO to have some notion of uncertainty in its probability predictions. Instead of predicting
222 1-0 probabilities we can scale the target class probabilities by the IOU of the predicted bounding
223 box with the ground truth box for a region. When YOLO predicts good bounding boxes it is also
224 encouraged to predict high class probabilities. For poor bounding box predictions it learns to predict
225 lower confidence probabilities.

226 We do not train to predict IOU from the beginning, only during the second stage of training. It is not
227 necessary for good performance but it does boost our mean average precision by 3-4%.
228

229 **2.3 Inference**
230

231 Just like in training, predicting detections for a test image only requires one network evaluation.
232 The network predicts 49 bounding boxes per image and class probabilities for each box. YOLO is
233 extremely fast at test time since it only requires a single network evaluation unlike classifier-based
234 methods.

235 The grid design enforces spatial diversity in the bounding box predictions. Often it is clear which
236 grid cell an object falls in to and the network only predicts one box for each object. However, some
237 large objects or objects near the border of multiple cells can be well localized by multiple cells. Non-
238 maximal suppression can be used to fix these multiple detections. While not critical to performance
239 as it is for R-CNN or DPM, non-maximal suppression adds 2-3% in mAP.
240

241 **2.4 Limitations of YOLO**
242

243 YOLO imposes strong spatial constraints on bounding box predictions since each grid cell only
244 predicts one box. This spatial constraint limits the number of nearby objects that our model can
245 predict. If two objects fall into the same cell our model can only predict one of them. Our model
246 struggles with small objects that appear in groups, such as flocks of birds.

247 Since our model learns to predict bounding boxes from data, it struggles to generalize to objects in
248 new or unusual aspect ratios or configurations. Our model also uses relatively coarse features for
249 predicting bounding boxes since our architecture has multiple downsampling layers from the input
250 image.

251 Finally, while we train on a loss function that approximates detection performance, our loss function
252 treats errors the same in small bounding boxes versus large bounding boxes. A small error in a large
253 box is generally benign but a small error in a small box has a much greater effect on IOU. Our main
254 source of error is incorrect localizations.
255

256 **3 Comparison to Other Detection Systems**
257

258 Object detection is a core problem in computer vision. Detection pipelines generally start by ex-
259 tracting a set of robust features from input images (Haar [19], SIFT [18], HOG [2], convolutional
260 features [3]). Then, classifiers [27, 16, 9, 7] or localizers [1, 23] are used to identify objects in the
261 feature space. These classifiers or localizers are run either in sliding window fashion over the whole
262 image or on some subset of regions in the image [26, 11, 28]. We compare the YOLO detection
263 system to several top detection frameworks, highlighting key similarities and differences.

264 **Deformable parts models.** Deformable parts models (DPM) use a sliding window approach to
265 object detection [7]. DPM uses a disjoint pipeline to extract static features, classify regions, predict
266 bounding boxes for high scoring regions, etc. Our system replaces all of these disparate parts with
267 a single convolutional neural network. The network performs feature extraction, bounding box
268 prediction, non-maximal suppression, and contextual reasoning all concurrently. Instead of static
269 features, the network trains the features in-line and optimizes them for the detection task. Our
unified architecture leads to a faster, more accurate model than DPM.

VOC 2012 test	mAP	aero	bike	bird	boat	bottle	bus	car	cat	chair	cow	table	dog	horse	mbike	person	plant	sheep	sofa	train	tv
MR.CNN.S.CNN [8]	70.7	85.0	79.6	71.5	55.3	57.7	76.0	73.9	84.6	50.5	74.3	61.7	85.5	79.9	81.7	76.4	41.0	69.0	61.2	77.7	72.1
DEEP.LENS.COCO	70.1	84.0	79.4	71.6	51.9	51.1	74.1	72.1	88.6	48.3	73.4	57.8	86.1	80.0	80.7	70.4	46.6	69.6	68.8	75.9	71.4
Fast R-CNN + YOLO	70.0	83.0	78.4	73.4	55.7	42.5	78.2	72.7	89.5	48.2	74.0	56.4	87.2	80.8	80.7	74.4	41.1	70.0	67.1	81.2	66.0
NoC [21]	68.8	82.8	79.0	71.6	52.3	53.7	74.1	69.0	84.9	46.9	74.3	53.1	85.0	81.3	79.5	72.2	38.9	72.4	59.5	76.7	68.1
Fast R-CNN [10]	68.4	82.3	78.4	70.8	52.3	38.7	77.8	71.6	89.3	44.2	73.0	55.0	87.5	80.5	80.8	72.0	35.1	68.3	65.7	80.4	64.2
NUS.NIN.C2000 [4]	63.8	80.2	73.8	61.9	43.7	43.0	70.3	67.6	80.7	41.9	69.7	51.7	78.2	75.2	76.9	65.1	38.6	68.3	58.0	68.7	63.3
BabyLearning [4]	63.2	78.0	74.2	61.3	45.7	42.7	68.2	66.8	80.2	40.6	70.0	49.8	79.0	74.5	77.9	64.0	35.3	67.9	55.7	68.7	62.6
R-CNN VGG BB [9]	62.4	79.6	72.7	61.9	41.2	41.9	65.9	66.4	84.6	38.5	67.2	46.7	82.0	74.8	76.0	65.2	35.6	65.4	54.2	67.4	60.3
NUS.NIN	62.4	77.9	73.1	62.6	39.5	43.3	69.1	66.4	78.9	39.1	68.1	50.0	77.2	71.3	76.1	64.7	38.4	66.9	56.2	66.9	62.7
R-CNN VGG [9]	59.2	76.8	70.9	56.6	37.5	36.9	62.9	63.6	81.1	35.7	64.3	43.9	80.4	71.6	74.0	60.0	30.8	63.4	52.0	63.5	58.7
Feature Edit [24]	56.3	74.6	69.1	54.4	39.1	33.1	65.2	62.7	69.7	30.8	56.0	44.6	70.0	64.4	71.1	60.2	33.3	61.3	46.4	61.7	57.8
YOLO	53.6	71.6	62.2	55.2	35.9	23.2	62.4	53.7	78.1	34.0	52.9	38.7	72.2	67.3	66.3	62.1	25.5	50.0	46.9	67.4	46.3
R-CNN BB [9]	53.3	71.8	65.8	52.0	34.1	32.6	59.6	60.0	69.8	27.6	52.0	41.7	69.6	61.3	68.3	57.8	29.6	57.8	40.9	59.3	54.1
SDS [12]	50.7	69.7	58.4	48.5	28.3	28.8	61.3	57.5	70.8	24.1	50.7	35.9	64.9	59.1	65.8	57.1	26.0	58.8	38.6	58.9	50.7
R-CNN [9]	49.6	68.1	63.8	46.1	29.4	27.9	56.6	57.0	65.9	26.5	48.7	39.5	66.2	57.3	65.4	53.2	26.2	54.5	38.1	50.6	51.6

Table 1: PASCAL VOC 2012 Leaderboard. YOLO compared with the full comp4 (outside data allowed) public leaderboard as of June 5th, 2015. Mean average precision and per-class average precision are shown for a variety of detection methods. YOLO is the top detection method that is not based on the R-CNN detection framework. Fast R-CNN + YOLO is one of the top methods overall, with a 1.6% boost over Fast R-CNN and the highest average precision in 6 out of 20 classes.

R-CNN. R-CNN and its variants use region proposals instead of sliding windows to find objects in images. These systems use region proposal methods like Selective Search [26] to generate potential bounding boxes in an image. Instead of scanning through every region in the window, now the classifier only has to score a small subset of potential regions in an image. Good region proposal methods maintain high recall despite greatly limiting the search space. This performance comes at a cost. Selective Search, even in “fast mode” takes about 2 seconds to propose regions for an image.

R-CNN shares many design aspects with DPM. After region proposal, R-CNN uses the same multi-stage pipeline of feature extraction (using CNNs instead of HOG), SVM scoring, non-maximal suppression, and bounding box prediction using a linear model [9].

YOLO shares some similarities with R-CNN. Each grid cell proposes a potential bounding box and then scores that bounding box using convolutional features. However, our system puts spatial constraints on the grid cell proposals which helps mitigate multiple detections of the same object. Our system also proposes far fewer bounding boxes, only 49 per image compared to about 2000 from Selective Search. Finally, our system combines these individual components into a single, jointly optimized model.

Deep MultiBox. Unlike R-CNN, Szegedy et al. train a convolutional neural network to predict regions of interest [5] instead of using Selective Search. MultiBox can also perform single object detection by replacing the confidence prediction with a single class prediction. However, MultiBox cannot perform general object detection and is still just a piece in a larger detection pipeline, requiring further image patch classification. Both YOLO and MultiBox use a convolutional network to predict bounding boxes in an image but YOLO is a complete detection pipeline.

OverFeat. Sermanet et al. train a convolutional neural network to perform localization and adapt that localizer to perform detection [23]. OverFeat efficiently performs sliding window detection but it is still a disjoint system. OverFeat optimizes for localization, not detection performance. Like DPM, the localizer only sees local information when making a prediction. OverFeat cannot reason about global context and thus requires significant post-processing to produce coherent detections.

Our work is most similar in design to work on grasp detection by Redmon et al [20].

4 Experiments

We present detection results for the PASCAL VOC 2012 dataset and compare our mean average precision (mAP) and runtime to other top detection methods. We also perform error analysis on the VOC 2007 dataset. We compare our results to Fast R-CNN, one of the highest performing versions of R-CNN [10]. We use publicly available runs of Fast R-CNN available on GitHub. Finally we show that a combination of our method with Fast R-CNN gives a significant performance boost.

324 **4.1 VOC 2012 Results**

325

326 On the VOC 2012 test set we achieve 53.6 mAP. This is lower than the current state of the art,
 327 closer to R-CNN based methods that use AlexNet, see Table 1. Our system struggles with small ob-
 328 jects compared to its closest competitors. On categories like `bottle`, `sheep`, and `tv/monitor`
 329 YOLO scores 8-10 percentage points lower than R-CNN or Feature Edit. However, on other cate-
 330 gories like `cat` and `horse` YOLO achieves significantly higher performance. We further investi-
 331 gate the source of these performance disparities in Section 4.3.

332 **4.2 Speed**

333

334 At test time YOLO processes images at 45 frames per second on an Nvidia Titan X GPU. It is
 335 considerably faster than classifier-based methods with similar mAP. Normal R-CNN using AlexNet
 336 or the small VGG network take 400-500x longer to process images. The recently proposed Fast
 337 R-CNN shares convolutional features between the bounding boxes but still relies on selective search
 338 for bounding box proposals which accounts for the bulk of their processing time. YOLO is still
 339 around 100x faster than Fast R-CNN. Table 2 shows a full comparison between multiple R-CNN
 340 and Fast R-CNN variants and YOLO.

	mAP	Prediction Time	FPS	Compared to YOLO
R-CNN (VGG-16)	66.0	48.2 hr	0.02 fps	1500x
FR-CNN (VGG-16)	66.9	3.1 hr	0.45 fps	100x
R-CNN (Small VGG)	60.2	14.4 hr	0.09 fps	500x
FR-CNN (Small VGG)	59.2	2.9 hr	0.48 fps	93x
R-CNN (Caffe)	58.5	12.2 hr	0.11 fps	409x
FR-CNN (Caffe)	57.1	2.8 hr	0.48 fps	93x
YOLO	58.8	110 sec	45 fps	-

350 **Table 2: Prediction Timing.** mAP and timing information for R-CNN, Fast R-CNN, and YOLO
 351 on the VOC 2007 test set. Timing information is given both as frames per second and the time each
 352 method takes to process the full 4952 image set. The final column shows the relative speed of YOLO
 353 compared to that method.

354

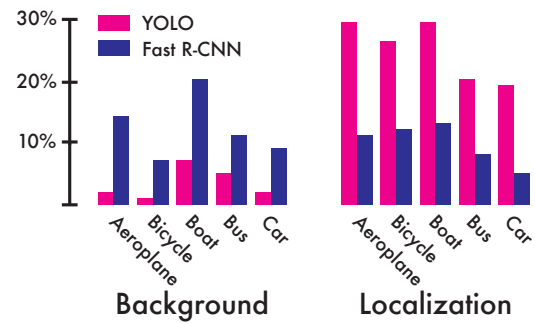
355 **4.3 VOC 2007 Error Analysis**

356

357 An object detector must have high recall for
 358 objects in the test set to obtain high perfor-
 359 mance. Our model imposes spatial constraints
 360 on bounding box predictions which limits re-
 361 call on small objects that are close together. We
 362 examine how detrimental this is in practice by
 363 calculating our highest possible recall assum-
 364 ing perfect coordinate prediction. Under this
 365 assumption, our model can achieve a 93.1% re-
 366 call for objects in the VOC 2007 test set. This
 367 is lower than Selective Search (98.0% [26]) but
 368 still relatively high.

369 Using the methodology and tools of Hoiem et
 370 al. [15] we analyze our performance on the
 371 VOC 2007 test set. We compare YOLO to Fast
 372 R-CNN using VGG-16, one of the highest per-
 373 forming object detectors.

374 Figure 4 compares frequency of localiza-
 375 tion and background errors between Fast R-CNN
 376 and YOLO. A detection is considered a local-
 377 ization error if it overlaps a true positive in the image but by less than the required 50% IOU. A
 378 detection is a background error if the box does not overlap any objects of any class in the image.



379 **Figure 4: Error Analysis: Fast R-CNN vs.**
YOLO These charts show the percentage of lo-
 380 calization and background errors in the top N de-
 381 tections for various categories (N = # objects in
 382 that category).

378 Fast R-CNN makes around the same number of localization errors and background errors. Over all
379 20 classes in the top N detections 13.6% are localization errors and 8.6% are background errors.
380

381 YOLO makes far more localization errors but relatively few background errors. Averaged across all
382 classes, of its top N detections 24.7% are localization errors and a mere 4.3% are background errors.
383 This is about twice the number of localization errors but half the number of background detections.

384 YOLO uses global context to evaluate detections while R-CNN only sees small portions of the
385 image. Many of the background detections made by R-CNN are obviously not objects when shown
386 in context. YOLO and R-CNN are good at different parts of object detection. Since their main
387 sources of error are orthogonal, combining them should produce a model that is better across the
388 board.

389 4.4 Combining Fast R-CNN and YOLO

390 YOLO makes far fewer background mistakes
391 than Fast R-CNN. By using YOLO to elimi-
392 nate background detections from Fast R-CNN
393 we get a significant boost in performance. For
394 every bounding box that R-CNN predicts we
395 check to see if YOLO predicts a similar box.
396 If it does, we give that prediction a boost based
397 on the probability predicted by YOLO and the
398 overlap between the two boxes. This reorders
399 the detections to favor those predicted by both
400 systems. Since we still use Fast R-CNN’s
401 bounding box predictions we do not introduce
402 any localization error. Thus we take advantage
403 of the best aspects of both systems.

404 The best Fast R-CNN model achieves a mAP of
405 71.8% on the VOC 2007 test set. When com-
406 bined with YOLO, its mAP increases by 2.9% to 74.7%. We also tried combining the top Fast
407 R-CNN model with several other versions of Fast R-CNN. Those ensembles produced small in-
408 creases in mAP between .3 and .6%, see Table 3 for details. Thus, the benefit from combining Fast
409 R-CNN with YOLO is unique, not a general property of combining models in this way.

410 Using this combination strategy we achieve a significant boost on the VOC 2012 and 2010 test sets
411 as well, around 2%. The combined Fast R-CNN + YOLO model performs on par with the best
412 models on the VOC 2012 leaderboard.

414 5 Conclusion

417 We introduce YOLO, a unified pipeline for object detection. Our model is simple to construct and
418 can be trained directly on full images. Unlike classifier-based approaches, YOLO is trained on a
419 loss function that directly corresponds to detection performance and every piece of the pipeline can
420 be trained jointly.

421 The network reasons about the entire image during inference which makes it less likely to predict
422 background false positives than sliding window or proposal region detectors. Moreover, it predicts
423 detections with only a single network evaluation, making it extremely fast.

425 YOLO achieves impressive performance on standard benchmarks considering it is 2-3 orders of
426 magnitude faster than existing detection methods. It can also be used to rescore the bounding boxes
427 produced by state-of-the-art methods like R-CNN for a significant boost in performance.

428 429 References

- 431 [1] M. B. Blaschko and C. H. Lampert. Learning to localize objects with structured output regression. In
Computer Vision–ECCV 2008, pages 2–15. Springer, 2008.

- [2] N. Dalal and B. Triggs. Histograms of oriented gradients for human detection. In *Computer Vision and Pattern Recognition, 2005. CVPR 2005. IEEE Computer Society Conference on*, volume 1, pages 886–893. IEEE, 2005.
- [3] J. Donahue, Y. Jia, O. Vinyals, J. Hoffman, N. Zhang, E. Tzeng, and T. Darrell. Decaf: A deep convolutional activation feature for generic visual recognition. *arXiv preprint arXiv:1310.1531*, 2013.
- [4] J. Dong, Q. Chen, S. Yan, and A. Yuille. Towards unified object detection and semantic segmentation. In *Computer Vision–ECCV 2014*, pages 299–314. Springer, 2014.
- [5] D. Erhan, C. Szegedy, A. Toshev, and D. Anguelov. Scalable object detection using deep neural networks. In *Computer Vision and Pattern Recognition (CVPR), 2014 IEEE Conference on*, pages 2155–2162. IEEE, 2014.
- [6] M. Everingham, S. M. A. Eslami, L. Van Gool, C. K. I. Williams, J. Winn, and A. Zisserman. The pascal visual object classes challenge: A retrospective. *International Journal of Computer Vision*, 111(1):98–136, Jan. 2015.
- [7] P. F. Felzenszwalb, R. B. Girshick, D. McAllester, and D. Ramanan. Object detection with discriminatively trained part based models. *IEEE Transactions on Pattern Analysis and Machine Intelligence*, 32(9):1627–1645, 2010.
- [8] S. Gidaris and N. Komodakis. Object detection via a multi-region & semantic segmentation-aware CNN model. *CoRR*, abs/1505.01749, 2015.
- [9] R. Girshick, J. Donahue, T. Darrell, and J. Malik. Rich feature hierarchies for accurate object detection and semantic segmentation. In *Computer Vision and Pattern Recognition (CVPR), 2014 IEEE Conference on*, pages 580–587. IEEE, 2014.
- [10] R. B. Girshick. Fast R-CNN. *CoRR*, abs/1504.08083, 2015.
- [11] S. Gould, T. Gao, and D. Koller. Region-based segmentation and object detection. In *Advances in neural information processing systems*, pages 655–663, 2009.
- [12] B. Hariharan, P. Arbeláez, R. Girshick, and J. Malik. Simultaneous detection and segmentation. In *Computer Vision–ECCV 2014*, pages 297–312. Springer, 2014.
- [13] K. He, X. Zhang, S. Ren, and J. Sun. Delving deep into rectifiers: Surpassing human-level performance on imagenet classification. *CoRR*, abs/1502.01852, 2015.
- [14] G. E. Hinton, N. Srivastava, A. Krizhevsky, I. Sutskever, and R. R. Salakhutdinov. Improving neural networks by preventing co-adaptation of feature detectors. *arXiv preprint arXiv:1207.0580*, 2012.
- [15] D. Hoiem, Y. Chodpathumwan, and Q. Dai. Diagnosing error in object detectors. In *Computer Vision–ECCV 2012*, pages 340–353. Springer, 2012.
- [16] R. Lienhart and J. Maydt. An extended set of haar-like features for rapid object detection. In *Image Processing. 2002. Proceedings. 2002 International Conference on*, volume 1, pages I–900. IEEE, 2002.
- [17] M. Lin, Q. Chen, and S. Yan. Network in network. *CoRR*, abs/1312.4400, 2013.
- [18] D. G. Lowe. Object recognition from local scale-invariant features. In *Computer vision, 1999. The proceedings of the seventh IEEE international conference on*, volume 2, pages 1150–1157. Ieee, 1999.
- [19] C. P. Papageorgiou, M. Oren, and T. Poggio. A general framework for object detection. In *Computer vision, 1998. sixth international conference on*, pages 555–562. IEEE, 1998.
- [20] J. Redmon and A. Angelova. Real-time grasp detection using convolutional neural networks. *CoRR*, abs/1412.3128, 2014.
- [21] S. Ren, K. He, R. B. Girshick, X. Zhang, and J. Sun. Object detection networks on convolutional feature maps. *CoRR*, abs/1504.06066, 2015.
- [22] O. Russakovsky, J. Deng, H. Su, J. Krause, S. Satheesh, S. Ma, Z. Huang, A. Karpathy, A. Khosla, M. Bernstein, A. C. Berg, and L. Fei-Fei. ImageNet Large Scale Visual Recognition Challenge. *International Journal of Computer Vision (IJCV)*, 2015.
- [23] P. Sermanet, D. Eigen, X. Zhang, M. Mathieu, R. Fergus, and Y. LeCun. Overfeat: Integrated recognition, localization and detection using convolutional networks. *CoRR*, abs/1312.6229, 2013.
- [24] Z. Shen and X. Xue. Do more dropouts in pool5 feature maps for better object detection. *arXiv preprint arXiv:1409.6911*, 2014.
- [25] C. Szegedy, W. Liu, Y. Jia, P. Sermanet, S. Reed, D. Anguelov, D. Erhan, V. Vanhoucke, and A. Rabinovich. Going deeper with convolutions. *CoRR*, abs/1409.4842, 2014.
- [26] J. R. Uijlings, K. E. van de Sande, T. Gevers, and A. W. Smeulders. Selective search for object recognition. *International journal of computer vision*, 104(2):154–171, 2013.
- [27] P. Viola and M. Jones. Robust real-time object detection. *International Journal of Computer Vision*, 4:34–47, 2001.
- [28] C. L. Zitnick and P. Dollár. Edge boxes: Locating object proposals from edges. In *Computer Vision–ECCV 2014*, pages 391–405. Springer, 2014.